

## Compatibility of lithium plasma-facing surfaces with high edge temperatures in the Lithium Tokamak Experiment (LTX)

R. Majeski, R. E. Bell, D. P. Boyle, R. Kaita, T. Kozub, B. P. LeBlanc, M. Lucia,<sup>i</sup> R. Maingi, E. Merino, Y. Raitses, J. C. Schmitt<sup>ii</sup>

*Princeton Plasma Physics Laboratory, Princeton, New Jersey 08543*

J. P. Allain, F. Bedoya

*University of Illinois, Urbana-Champaign, Illinois 61801*

J. Bialek

*Columbia University, New York, New York 10027*

T. M. Biewer, J. M. Canik

*Oak Ridge National Laboratory, Oak Ridge, Tennessee 37831*

L. Buzi, B. E. Koel, M. I. Patino

*Princeton University, Princeton, New Jersey 08544*

A. M. Capece

*The College of New Jersey, Ewing, New Jersey 08618*

C. Hansen, T. Jarboe

*University of Washington, Seattle, Washington 98105*

S. Kubota, W. A. Peebles

*University of California at Los Angeles, Los Angeles, California 90095*

K. Tritz

*Johns Hopkins University, Baltimore, Maryland 21218*

**Abstract** High edge electron temperatures (200 eV or greater) have been measured at the wall-limited plasma boundary in the Lithium Tokamak Experiment (LTX). Flat electron temperature profiles are a long-predicted consequence of low recycling boundary conditions. Plasma density in the outer scrape-off layer is very low,  $2\text{-}3 \times 10^{17} \text{ m}^{-3}$ , consistent with a low recycling metallic lithium boundary. Despite the high edge temperature, the core impurity content is low.  $Z_{\text{eff}}$  is estimated to be  $\sim 1.2$ , with a very modest contribution ( $<0.1$ ) from lithium. Experiments are transient. Gas puffing is used to increase the plasma density. After gas injection stops, the discharge density is allowed to drop, and the edge is pumped by the low recycling lithium wall. An upgrade to LTX – LTX- $\beta$  – which includes a 35A, 20 kV neutral beam injector (on loan to LTX from Tri-Alph Energy) to provide core fueling to maintain constant density, as well as auxiliary heating, is underway. LTX- $\beta$  is briefly described.

<sup>i</sup> Present address: Lockheed Martin Corporation, Cherry Hill, New Jersey 08002

<sup>ii</sup> Present address: Auburn University, Auburn, Alabama 36849

## I. Introduction

The Lithium Tokamak eXperiment (LTX) is a low aspect ratio tokamak with  $R=0.4$  m,  $a=0.26$  m, and  $\kappa=1.5$ . Typical parameters are  $B_{\text{toroidal}} \sim 1.7$  kG,  $I_p < 85$  kA (60 kA in the discharges considered here), and a discharge duration  $< 50$  msec. LTX features a conformal 1 cm thick copper shell or liner. The plasma-facing surface of the shell is clad with explosively bonded 1.5 mm thick 304 stainless steel. Prior to a day's operations, the stainless steel cladding is coated with lithium to form the plasma-facing surface. The shell conforms to the last closed flux surface (LCFS) for a plasma with the nominal geometric parameters specified above, covers 80% of the plasma surface area, and can be electrically heated to 350 °C. LTX was designed to investigate modifications to tokamak equilibrium caused by low recycling lithium walls.

## II. Results with lithium walls after the termination of gas puff fueling

Discharges with high edge electron temperatures and flat radial electron temperature profiles – an isothermal confined electron population – have now been achieved in LTX<sup>1</sup> with lithium plasma-facing surfaces. Experiments use a lithium coating system which employs both electrical heating of the shell system, and additional electron beam heating to evaporate two lithium pools in the lower shell structure. The lithium pools are heated to  $\sim 500$  °C for 10 – 20 minutes. Each heating cycle evaporates up to a few hundred milligrams of lithium, to produce 10 – 100 nm thick coatings over the entire plasma-facing surface. A more complete description of LTX and the lithium coating system has been previously published.<sup>2</sup> Very low levels of residual water in the device (partial pressures in the mid to upper  $10^{-10}$  Torr range) assist in maintaining lithium surface conditions. The surface composition of lithium coatings in LTX has been analyzed with post-discharge X-ray photoelectron spectroscopy (XPS) using the MAPP (Materials Analysis and Particle Probe<sup>3</sup>), which indicates that the principal surface contaminant is oxygen. Initially the lithium-oxygen ratio in the surface is  $\sim 8:1$ ; over a period of  $\sim 10$  hours (longer than a run-day) the oxygen content of the surface increases until the lithium-oxygen ratio approaches 2:1, which is indicative of the formation of lithium oxide.<sup>4</sup> XPS is a surface-localized diagnostic technique which accesses the elemental composition to a depth of 3 nm. In order to oxidize the entire 100

ing coating of lithium which is typically applied to the LTX plasma-facing surfaces, several days of exposure to background vacuum conditions would be required.

The only fueling approach available in LTX is gas puffing, with a gas nozzle located on the high field side midplane of the centerstack assembly. In order to eliminate neutral fueling gas for part of the LTX discharge, the plasma density is initially increased with gas puffing to a line averaged density of approximately  $7 \times 10^{18} \text{ m}^{-3}$ . Gas injection is then terminated at  $t = 465 \text{ msec}$ , and the

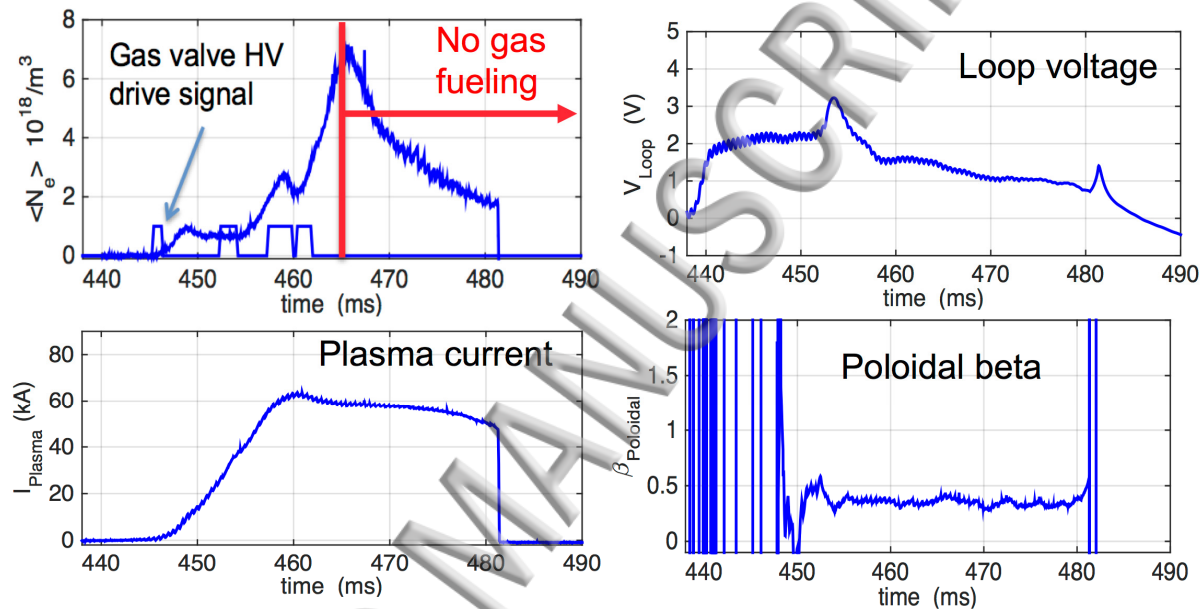


Figure 1. Time evolution of the line density (with the gas puffing intervals indicated), the loop voltage, the plasma current, and the poloidal beta during the experiment. The 55 discharges used for the experimental database were very reproducible.<sup>1</sup>

discharge density is allowed to drop, while the remaining edge neutral population fuels the discharge, and is in turn pumped by the lithium wall over the following 3-5 msec. During this period, the edge neutral gas pressure drops into the low  $10^{-5}$  to upper  $10^{-6}$  Torr range. Figure 1 shows the temporal evolution of the line-averaged density (with gas puffing indicated), as well as the evolution of the plasma current, the loop voltage, and the poloidal beta during the experiment. The plasma current is held as constant during the latter phase of the discharge as the control system permits.

the neutral gas in the edge is pumped, the electron temperature profile evolves from broad, but still peaked on axis, with an edge temperature of  $\sim 50$  eV at the LCFS (similar to earlier discharges in LTX, which exhibited relatively flat core electron temperature profiles out to  $r/a \sim 0.7-0.8$ , dropping to 20-30 eV at the LCFS<sup>5</sup>), to a very flat profile with an edge temperature  $> 200$  eV. Flat temperature profiles extending to the bounding wall have been predicted to be a consequence of low recycling boundary conditions,<sup>6</sup> but have not been previously observed in any magnetic confinement device. Temperature profiles in LTX are measured in discharges with

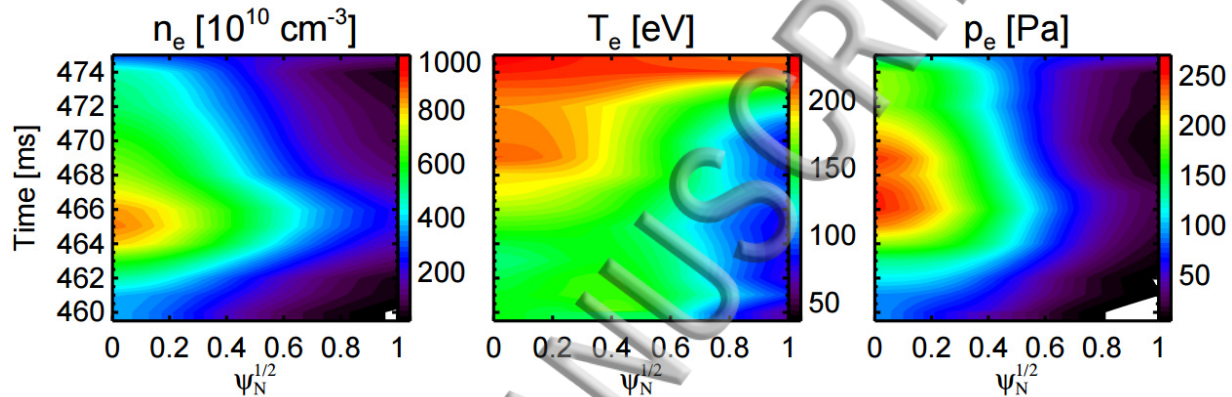


Figure 2. (Color) Contour plots of the evolution of the electron density, temperature, and pressure profiles in LTX. Gas puffing is terminated at 465 msec. 3-5 msec are required to clear hydrogen gas from the feedlines, at which point there is neither puffed gas nor a significant recycled gas component in the plasma edge. Low recycling and the lack of cold gas leads to nearly complete flattening of the electron temperature profile by 474 msec in the discharge. At the same time, the edge plasma density in the scrape-off layer drops to  $2-3 \times 10^{17} \text{ m}^{-3}$ . The pressure profile broadens, despite peaking in the density profile. Note that the plasma is initiated at 445 msec.

multipoint, single-pulse Thomson scattering. The evolution of the electron temperature profile was determined by stepping the measurement time through the discharge, and averaging the data over several discharges for each time point (especially for the low density edge), using a set of 55 identical discharges obtained within a single run day, following a fresh lithium coating cycle. The evolution of the electron temperature, density, and pressure is shown in Figure 2.

The temporal evolution of the edge and core electron temperature and density are shown in Figure 3. The core temperature rises gradually once gas puffing is terminated, from 150 eV to  $> 200$  eV. However, the edge temperature increases by nearly a factor of five from 470 to 474 msec. Four milliseconds is 2-3 confinement times for this discharge. The core and edge electron

density both drop after gas puffing is terminated, but whereas the core density drops by approximately 40% over the last 8 msec of displayed data, the edge density drops by approximately an order of magnitude.

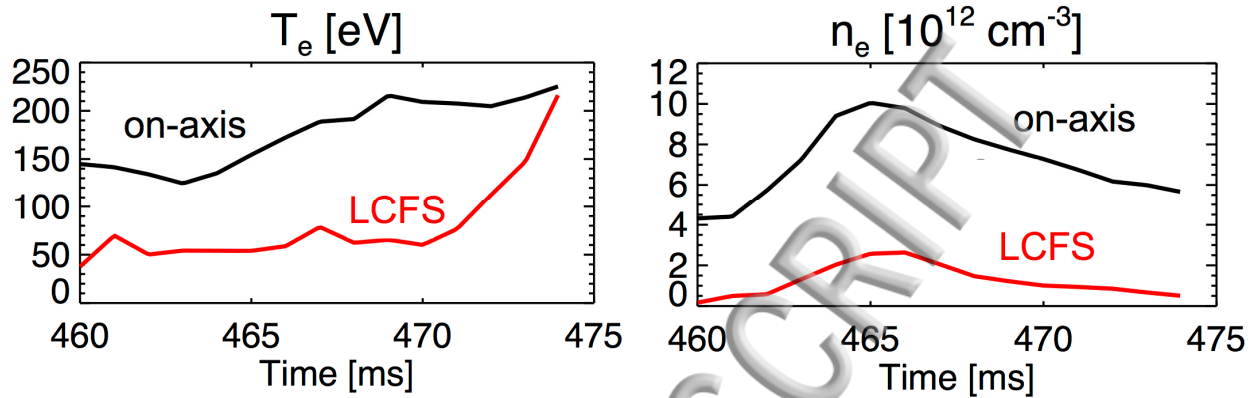


Figure 3. Evolution of the edge and core electron temperature and density during the discharge. The positions of the axis and LCFS are from spline fit Thomson scattering profiles mapped onto the equilibrium using the TRANSP code.

A more detailed comparison of the radial electron temperature profiles just after gas puffing is terminated (at  $t=464.9$  msec), during the edge temperature rise at  $t=472.9$  msec, and after the edge temperature has risen to match the core temperature, at  $t = 474$  msec, is shown in Figure 4.

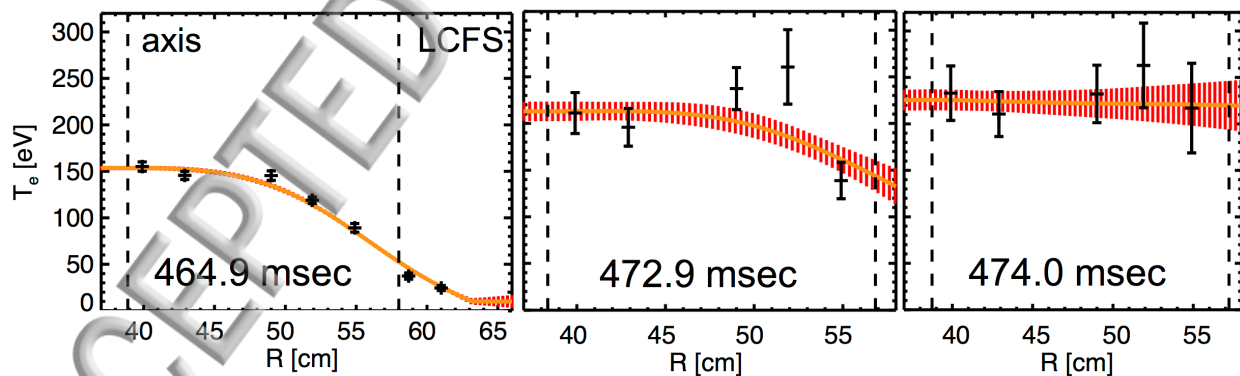


Figure 4. Radial plots of the electron temperature near the end of gas puff fueling in LTX (464.9 msec), during the edge temperature rise at 472.9 msec, and after the temperature profile has flattened at 474.0 msec. The position of the last closed flux surface is determined by magnetic equilibrium reconstruction with the PSI-TRI code.<sup>7</sup> An alternate determination of the position of the LCFS, from direct magnetic measurements,<sup>8</sup> would indicate that the position of the LCFS is 1 - 2 cm inboard of the position shown in the plots in Figure 4.



Although the density profile remains peaked during the period when the electron temperature profile flattens (see Figure 2), the combined effect of density and temperature profile evolution is to slightly broaden the electron pressure profile, as can also be seen in Figure 2.

Analysis with the TRANSP code,<sup>9</sup> supported by spectroscopic measurements of impurity ion temperatures, indicates that the ion temperature are 40 – 70 eV, and the profiles are also flat. The density profile decreases approximately linearly with the poloidal flux, to a very low edge density of  $2\text{-}3 \times 10^{17} \text{ m}^{-3}$ . The core impurity content, even in low density plasmas without hydrogen fueling, and edge electron temperatures of 200 eV, is estimated to be low, using visible spectroscopy and a simple model for unmeasured charge states.<sup>10</sup>  $Z_{\text{eff}}$  is approximately 1.2, with most of the increase from oxygen, followed by carbon. The smallest fraction of the  $Z_{\text{eff}}$  increase, especially in the core, is from lithium. The contribution to  $Z_{\text{effective}}$  for lithium, carbon, and oxygen is shown in Figure 5. Low lithium content in the core plasma has also been observed with lithium coatings in NSTX<sup>11</sup> and in TFTR,<sup>12</sup> but partial lithium coverage of the graphite walls

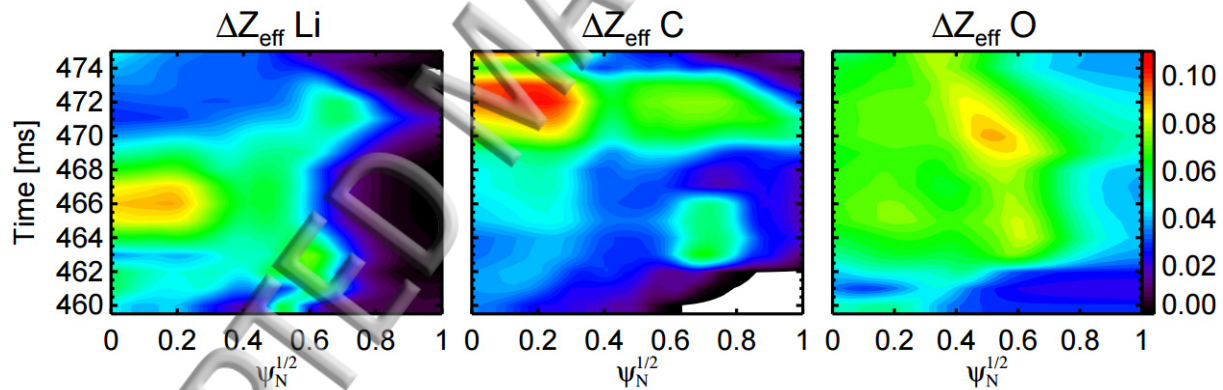


Figure 5. (Color) Contour plots of the evolution of the contribution of lithium, carbon, and oxygen to the discharge  $Z_{\text{effective}}$  in LTX. The lithium atomic concentration was 2-4%, carbon  $\sim 0.4\%$ , and oxygen  $\sim 0.7\%$ .

in those devices led to an accumulation of carbon in the core plasma. In NSTX, this was especially true during the inter-ELM period in the discharge. In LTX, the substrate for the lithium coating is metallic, and the carbon and oxygen content originates only from residual background gases in the vacuum chamber. The contribution of carbon to  $Z_{\text{effective}}$  remains  $\leq 0.1$ .

Other results from LTX include successful operation with full liquid lithium walls, 4 m<sup>2</sup> in area, covering >80% of the plasma surface area, and forming all of the plasma-facing components (PFCs), with wall temperatures up to 270 °C.<sup>2</sup> Similar impurity levels are seen in these discharges, with  $Z_{\text{effective}}$  remaining below 1.5, which demonstrates the compatibility of tokamak operation with liquid lithium PFCs. It is important to note that with an edge electron temperature in the range of 200 – 300 eV, the wall sheath potential for a conventional Debye sheath, and

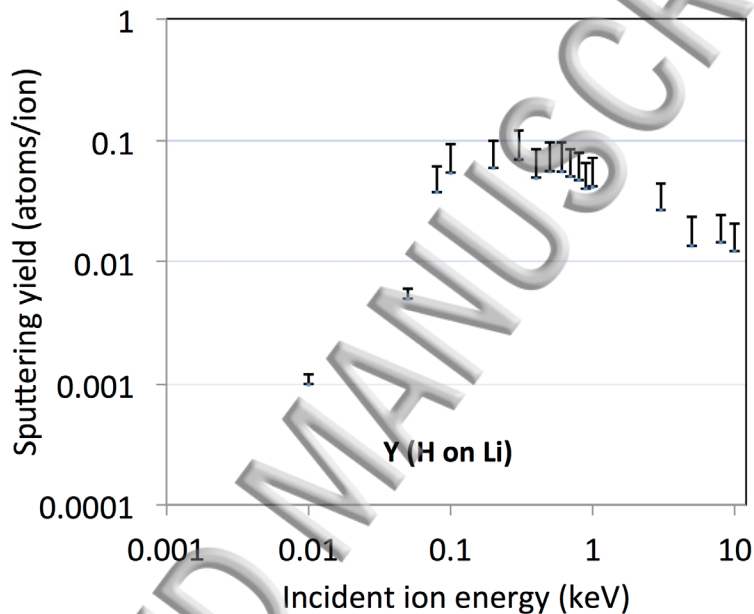


Figure 6. TRIM calculation of the sputtering yield for proton impact on lithium, at normal incidence. The yield peaks at somewhat below 1 keV energy.

hence the ion impact energy on the wall, will approach 1 kV. This is somewhat in excess of the peak sputtering energy for hydrogen impact on lithium, shown in Figure 6, but still – for LTX with high edge electron temperatures - very near the peak in sputtering yield. Further increases in the edge electron temperature, and consequently the Debye sheath, should lead to a decrease in lithium impurity influx. At very high edge temperatures (typical of a reactor), similar calculations indicate that the sputtering yield for deuteron impact on lithium will be very small.<sup>13</sup>

Discharges in LTX are limited on the lithium-coated high field side wall, and collisionality in the outer, low field side SOL is very low, with  $v_{i,e}^* < 0.1$  from the half-radius out, and approaching 0.01 in the edge during the period when the temperature profiles are flattened. Collisionality as a function of time through the discharge for ions and electrons is shown in Figure 7.

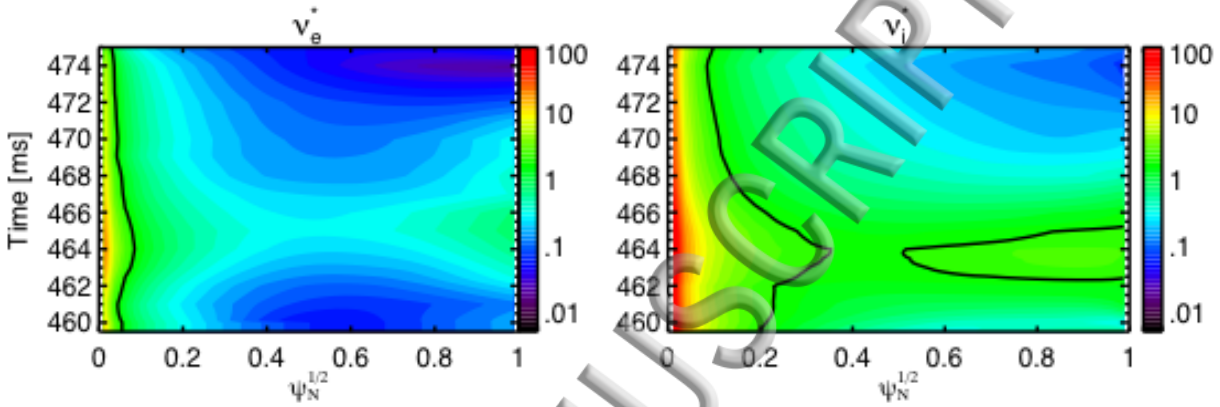


Figure 7. (Color) Collisionality for ions and electrons as a function of time in the discharge. The solid lines denote the boundary between the banana and plateau regimes. The discharge is almost entirely in the banana regime for both electron and ions during the period when electron temperatures are flat.

There is a significant gap between the outboard last closed flux surface and the outer lithium-coated shell surface, as indicated in Figure 8. These discharges were operated at moderately low plasma current ( $\sim 60$  kA in the flattop, with  $q(a) \sim 5$ ). Since the edge neutral pressure is in the high  $10^{-6}$  Torr range, the mean free path for ion charge exchange is  $> 1$  km. Since LTX is a low aspect ratio tokamak, the mirror ratio from the outboard LCFS to the high field side limiting surface is  $\sim 4$ , and increases further into the SOL. As a result, 80 – 90% of the particles in the outboard SOL are trapped. In the absence of charge exchange losses, and if radial transport is neglected, the principle mechanism for particle loss from the outboard SOL plasma is pitch angle scattering onto passing orbits. The pitch angle scattering time for the relatively hot electron population is  $\tau_{ee} \sim 400$   $\mu$ sec, and for the cooler ions  $\tau_{ii} \sim 1$  -2 msec. Since the connection length from the outboard midplane to the inboard limiting surface is  $L_{\text{conn}} \sim 5$  m, the pitch angle scattering times for either electrons or ions are longer than the flow time to the limiting surface ( $L_{\text{conn}}/C_s$ ), where  $C_s$  is the sound speed. The SOL plasma is therefore effectively mirror trapped, and in order to ensure ambipolarity of losses, must develop a positive Pastukhov (ambipolar)



potential  $\phi_p$ , for the ion and electron loss rates to be equal. Since  $T_e > T_i$ , this potential is relatively modest,<sup>14</sup> with  $\phi_p$  approximately  $0.6 - 0.8 kT_e$ . Unlike the SOL sheath potential, however, which is confined to a region very near the limiting surface in a limited tokamak, or to the private flux region in a diverted tokamak, the Pastukhov potential should extend into the low field side equatorial region, and may have a role in ejecting low energy sputtered impurities from the SOL in LTX. Note that although edge temperatures and densities have been measured with Thomson scattering, adequate diagnostics to measure the space potential and other SOL parameters in LTX was not available. Greater emphasis is being placed on SOL diagnostics for LTX- $\beta$ .

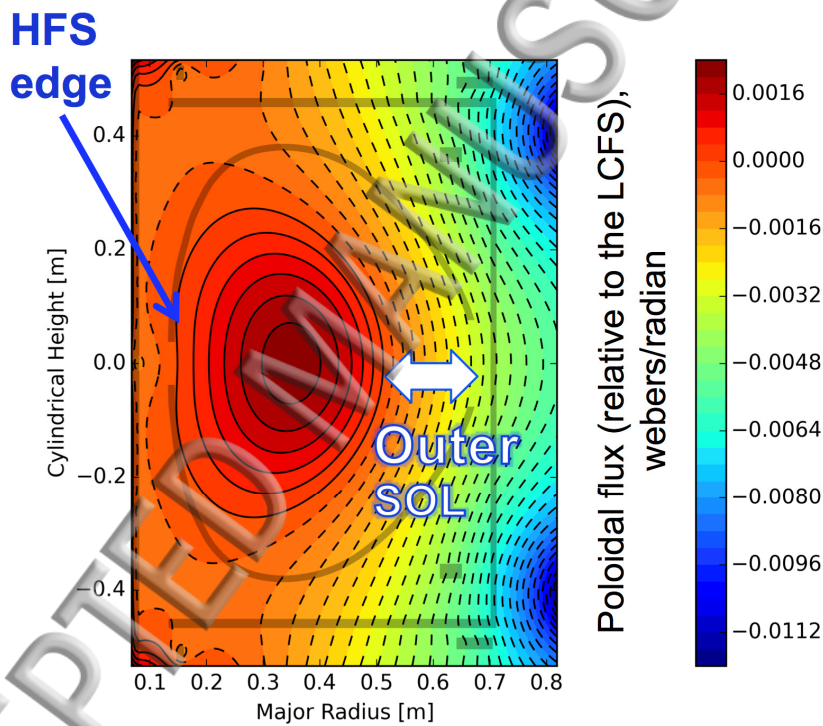


Figure 8. (Color) Equilibrium reconstruction of the LTX plasma with the PSI-TRI code, which includes corrections for the magnetic field components produced by the eddy currents induced in the copper shell structure by time-varying poloidal fields. The distance between the outer LCFS and the shell-defined wall is approximately 10 cm, at times late in the discharge when the electron temperature profile is fully flat.

The development of a broad low field side SOL is attributed in part to large ion orbit widths in the low toroidal field, low Ohmic current LTX discharge. The ion poloidal gyroradius for 40 - 70

hydrogen is 2 - 3 cm. The observed gap between the LCFS and the outer lithium-coated shell surface is 10 cm, or a few ion poloidal gyroradii (see Figure 8). High ion temperatures at the edge of a low recycling lithium tokamak have strong implications for edge power flow in a tokamak reactor.

Since the temperature is flat to the wall, the implied temperature decay length in the SOL is very long. Since the ion temperature at the edge is high, the density scrape-off length, which must exceed the ion poloidal gyroradius by at least a modest factor, must be long (as is experimentally observed in LTX). This implies that the divertor power footprint in a low recycling tokamak will be much broader than for a high recycling machine, possibly eliminating the need for advanced divertor configurations such as the snowflake or super-X divertors. In addition to SOL broadening through increase of the temperature scrape-off length and the poloidal ion gyroradius, the SOL width may be significantly increased by edge turbulence.<sup>15</sup> In the case of a collisionless SOL, e.g. for LTX, or for a future reactor, the plasma loss rate along field lines from the SOL is determined not by simple flow, with a characteristic loss time ( $L_{\text{conn}}/C_s \sim 60 \mu\text{sec}$ ), but by ion pitch angle scattering, with a characteristic time  $\tau_{\text{ii}} \sim 1 - 2 \text{ msec} \gg (L_{\text{conn}}/C_s)$ , for LTX. The longer SOL confinement times would significantly increase the efficacy of turbulent broadening of the SOL, for a given level of turbulence.

Of course, maintenance of a very low recycling edge is incompatible with puffing a radiating gas such as neon or nitrogen. There are as yet no scalings for the power deposition profile in a low recycling tokamak; future experiments in LTX- $\beta$  will investigate this for the first time.

### III. The upgrade to LTX: LTX- $\beta$

In late 2015 LTX was vented in preparation for an upgrade to LTX- $\beta$ . LTX- $\beta$  will feature neutral beam injection, using one of two neutral beams loaned to the LTX group by Tri-Alpha Energy, a private company investigating FRC-based fusion concepts in Foothills Ranch, CA. The planned installation of the neutral beam on LTX- $\beta$  is shown in Figure 9. The neutral beam will be operated at 17 - 20 kV, with up to 35 A in injected current, in hydrogen. The initial operating pulse will be power supply limited to 8 msec, with a subsequent doubling of the pulse length,

through the use of both available neutral beam power supplies. Another doubling of the pulse length is planned, with an expansion of the existing power supplies, to a total of 30 msec. The beam will provide both heating and partial fueling of the core plasma, which will reduce the need for gas-puff fueling. A collaboration with Oak Ridge National Laboratory will provide

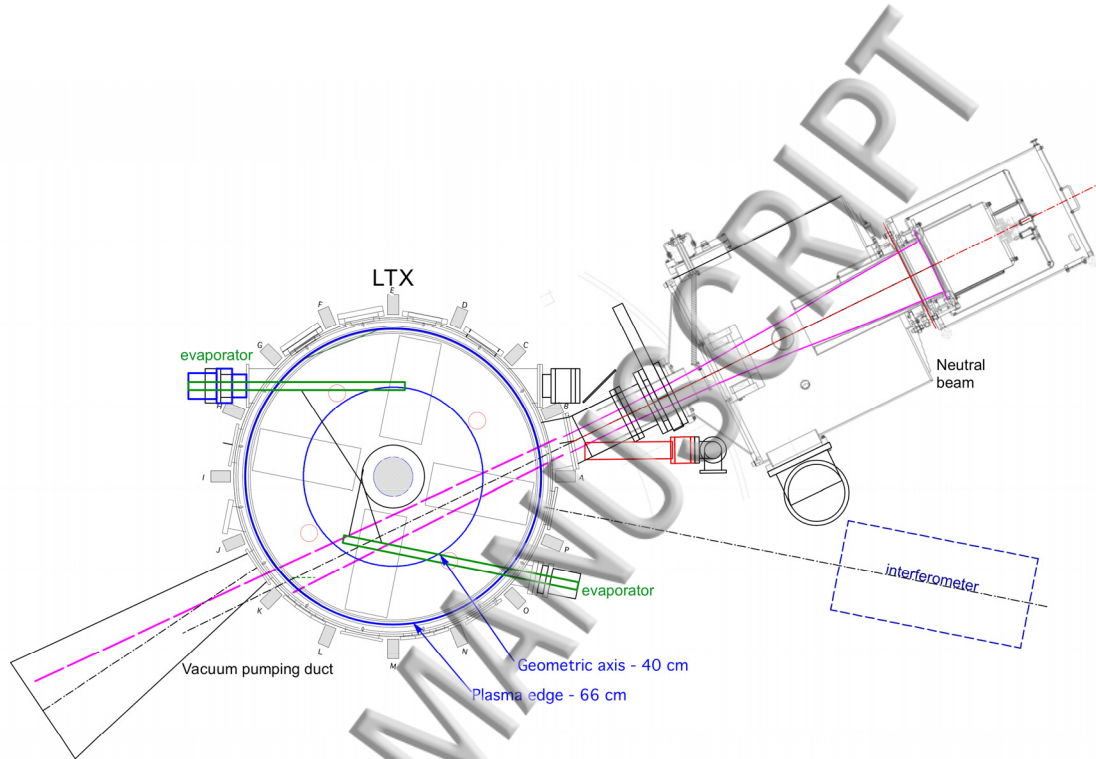


Figure 9. Layout of the neutral beam installation on LTX.

beam-based core plasma diagnostics, in particular CHERS (Charge Exchange Recombination Spectroscopy). The CHERS diagnostic will also provide measurements of the plasma rotation profile, and toroidal momentum transport in the absence of neutral drag. A collaboration with the University of California at Los Angeles will upgrade the existing microwave profile reflectometer diagnostic to record core density fluctuations. A new edge detector array for the Thomson scattering system will be completed, and, as stated previously, SOL diagnostics will be expanded. Additionally, the toroidal field is being doubled to 3.5 kG, and the plasma current will be increased to 150 – 200 kA.

#### IV. Summary

Experiments in LTX have demonstrated several key features of the lithium tokamak.

1. The production of flat temperature profiles – an “Isothermal Tokamak” or “Isomak” discharge.<sup>16</sup> The absence of recycled gas (and significant radiative losses) in the edge removes the mechanisms by which a confined plasma is cooled in the SOL and edge. Confined particles which exit the plasma only lose energy in the lithium wall itself. The thermal gradient, which drives conduction losses, should be robustly eliminated, regardless of changes in the particle transport, so long as another cooling mechanism is not introduced into the edge.

2. Core impurity control with low-Z walls. The use of lithium coatings which entirely overlay a high-Z substrate results in modest core impurity content, despite very high ion impact energies, produced by a hot SOL. High ion impact energies are unacceptable with solid high-Z PFCs, such as tungsten, since significant surface damage to the PFC would result, as well as sputtering of high-Z impurities into the plasma. The surface of a liquid cannot be damaged by ion impact. With lithium walls, a transition to higher ion energies would result in decreased transfer of energy to surface atoms, and decreased sputtering, as shown in simulations.

3. The development of a collisionless scrape-off layer. The low edge density, the lack of charge exchange losses due to recycled gas, and the high mirror ratio in a low aspect ratio tokamak imply that ion trapping in the SOL is dominant. The time scale for pitch angle scattering of the ions from trapped to passing orbits is long compared to the flow time ( $C_{\text{sound}}/L_{\text{connection}}$ ) to the wall, which will significantly modify the SOL in a lithium tokamak. In addition, the absence of a SOL temperature gradient, and the increased ion poloidal gyroradius, contribute to a significant broadening of the SOL scale length for power deposition.

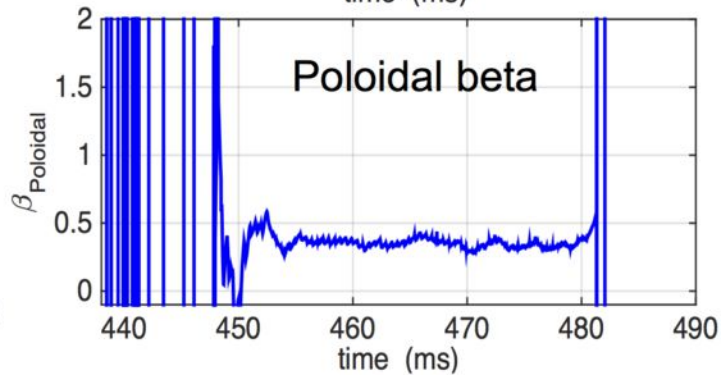
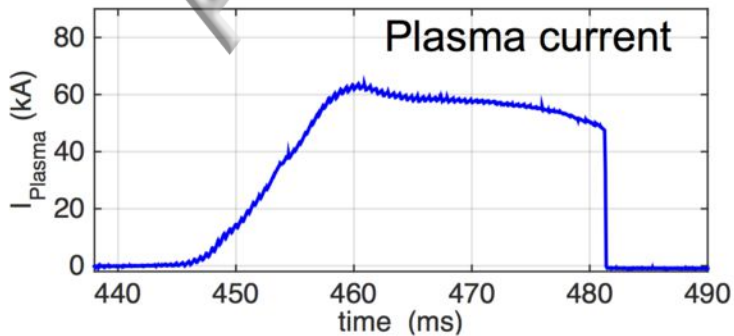
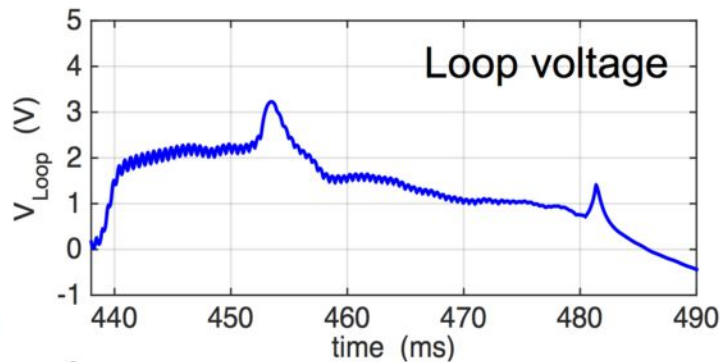
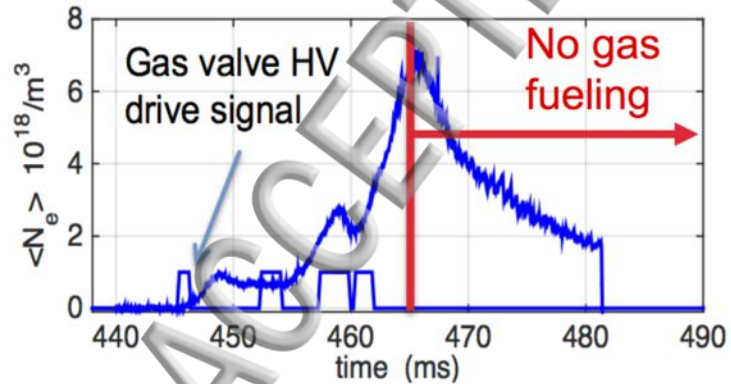
#### V. Acknowledgments

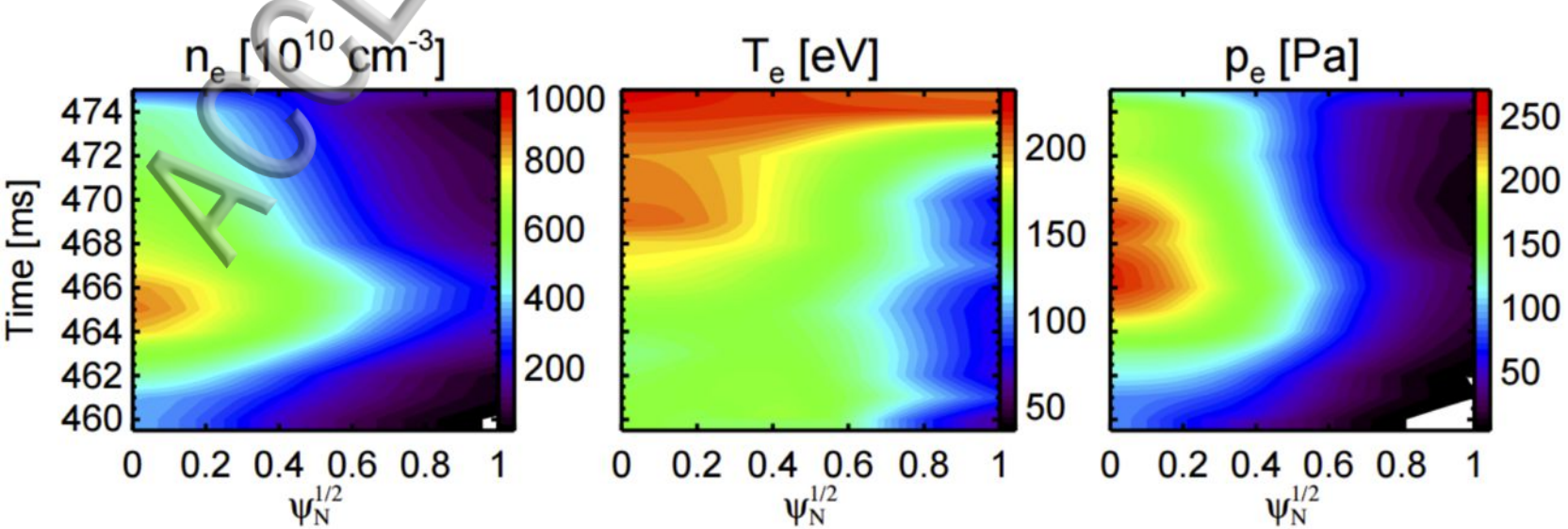
This work was supported by USDoE contracts DE-AC02-09CH11466 and DE-AC05-00OR22725. The digital data for this paper can be found at <http://arks.princeton.edu/ark:/88435/dsp01x920q025r>

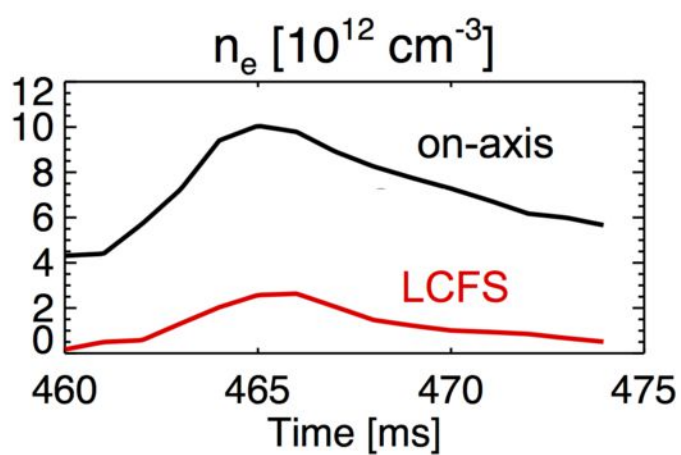
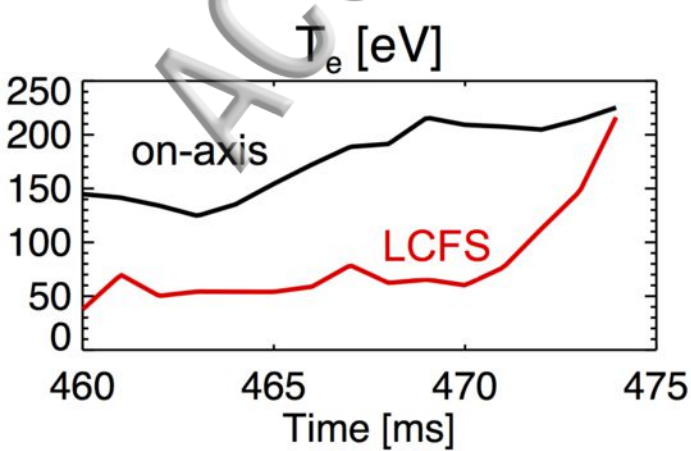
References

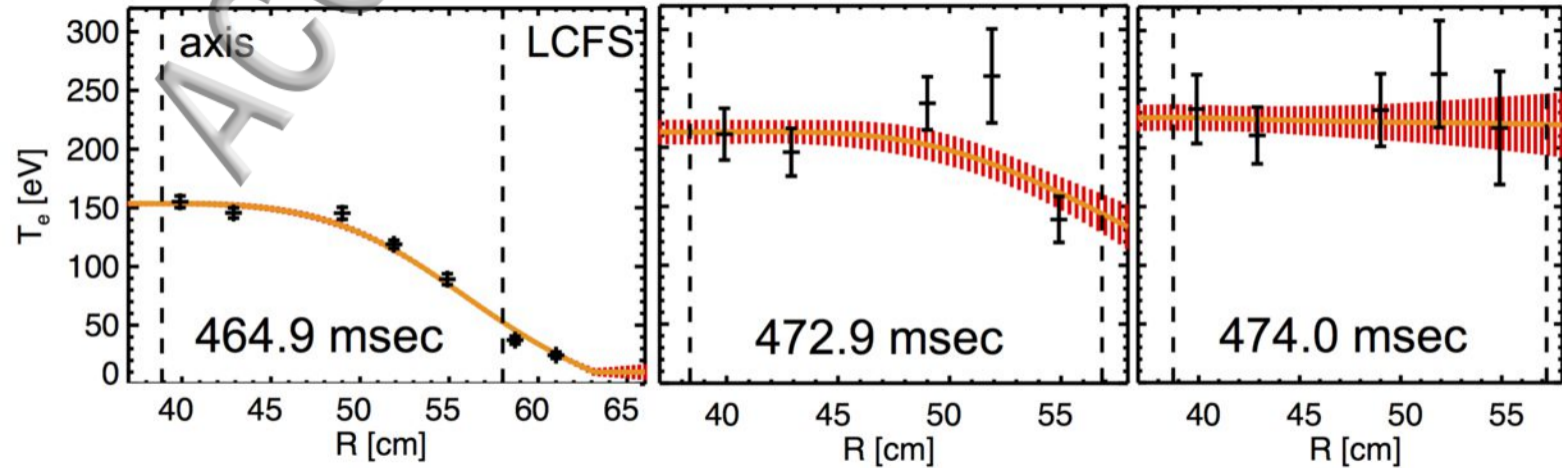
- <sup>1</sup> D. P. Boyle, R. Majeski, J. C. Schmitt, C. Hansen, R. Kaita, S. Kubota, M. Lucia, "Observation of flat electron temperature profiles in the Lithium Tokamak Experiment," submitted to Phys. Rev. Lett.
- <sup>2</sup> J. C. Schmitt, R. E. Bell, D. P. Boyle, B. Esposti, R. Kaita, B. P. LeBlanc, M. Lucia, R. Maingi, R. Majeski, et al., Phys. Plasmas **22**, 056112 (2015).
- <sup>3</sup> M. Lucia, R. Kaita, R. Majeski, F. Bedoya, J. P. Allain, T. Abrams, R. Bell, D. Boyle, M. Jaworski, J. Schmitt, J. Nucl. Mat. **463**, 907 (2015).
- <sup>4</sup> M. Lucia, Ph. D thesis, Princeton University, September 2015.
- <sup>5</sup> R. Majeski, T. Abrams, L. R. Baylor, L. Berzak, T. Biewer, D. Bohler, D. Boyle, M. Cassin, E. Granstedt, T. Gray, et al., "Results from LTX with Lithium-Coated Walls," Proc. 24th IAEA Fusion Energy Conference, San Diego, 2012, paper ICC/P5-01.
- <sup>6</sup> S. Krasheninnikov, L. Zakharov, and G. Pereverzev, Phys. Plasmas **10**, 1678(2003).
- <sup>7</sup> C. Hansen, J. Levesque, J. Bialek, D. P. Boyle, J. C. Schmitt, Bull. Am. Phys. Soc. **61**, GP10.00105 (2016).
- <sup>8</sup> I. H. Hutchinson, "Principles of Plasma Diagnostics," 2<sup>nd</sup> ed., (Cambridge University Press, Cambridge, 2002) p. 24.
- <sup>9</sup> R. Hawryluk, in "Physics of Plasmas Close to Thermonuclear Conditions," Volume 1, Proceedings of the Course Held in Varenna, Italy, 27 August – 8 September 1979, edited by B. Coppi, G. G. Leotta, D. Pfirsch, R. Pozzoli, and E. Sindoni (Elsevier, Amsterdam, 1981), p. 19.
- <sup>10</sup> D. P. Boyle, Ph. D. thesis, Princeton University, September 2016.
- <sup>11</sup> F. Scotti, V. A. Soukhanovskii, R. E. Bell, S. Gerhardt, W. Guttenfelder, S. Kaye, R. Andre, A. Diallo, R. Kaita, B. P. LeBlanc, M. Podesta and the NSTX team, Nucl. Fusion **53**, 083001(2013).
- <sup>12</sup> D. K. Mansfield, D. W. Johnson, B. Grek, H. W. Kugel, M. G. Bell, R. E. Bell, R. V. Budny, C. E. Bush, E. D. Fredrickson, K. W. Hill, et al., Nucl. Fusion **41**, 1823 (2001).
- <sup>13</sup> J. Laszlo and W. Eckstein, "Sputtering and reflection from lithium, gallium and indium," J. Nuc. Mater. **184**, 22(1991).
- <sup>14</sup> V. P. Pastukhov, Nuc. Fusion **14**, 3 (1974).
- <sup>15</sup> J. R. Myra, D. A. Russell, and S. J. Zweben, Phys. Plasmas **23**, 112502 (2016).
- <sup>16</sup> P. Catto and R. Hazeltine, "Isothermal tokamak," Phys. Plasmas **13**, 122508 (2006).

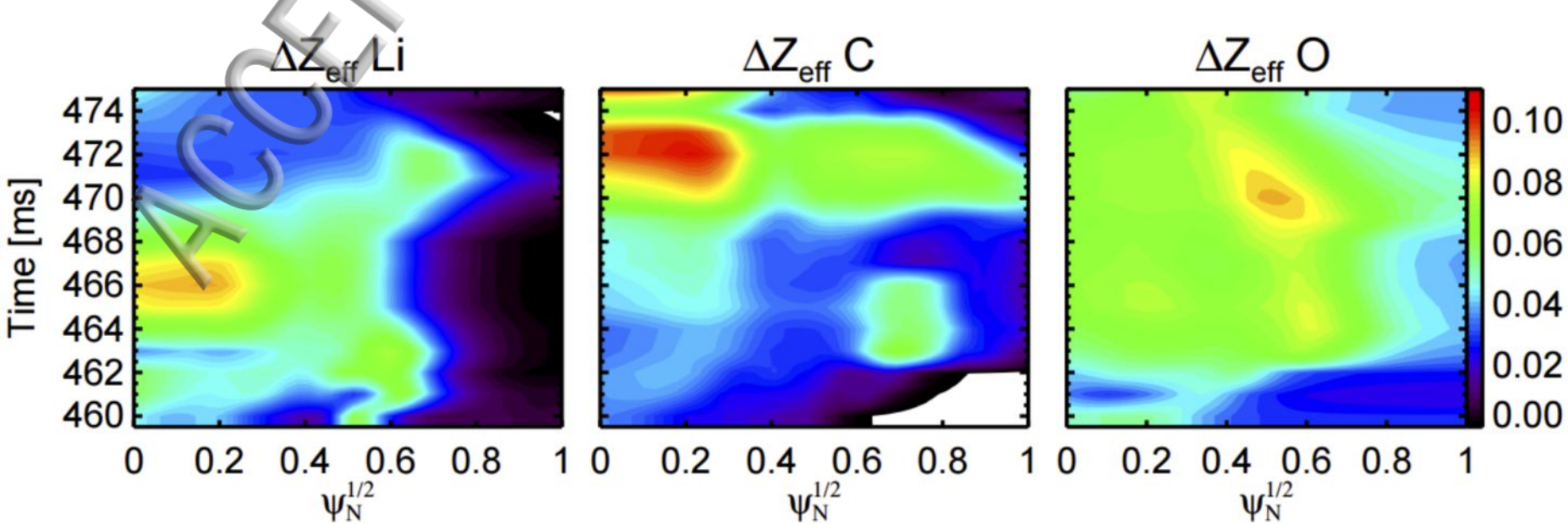




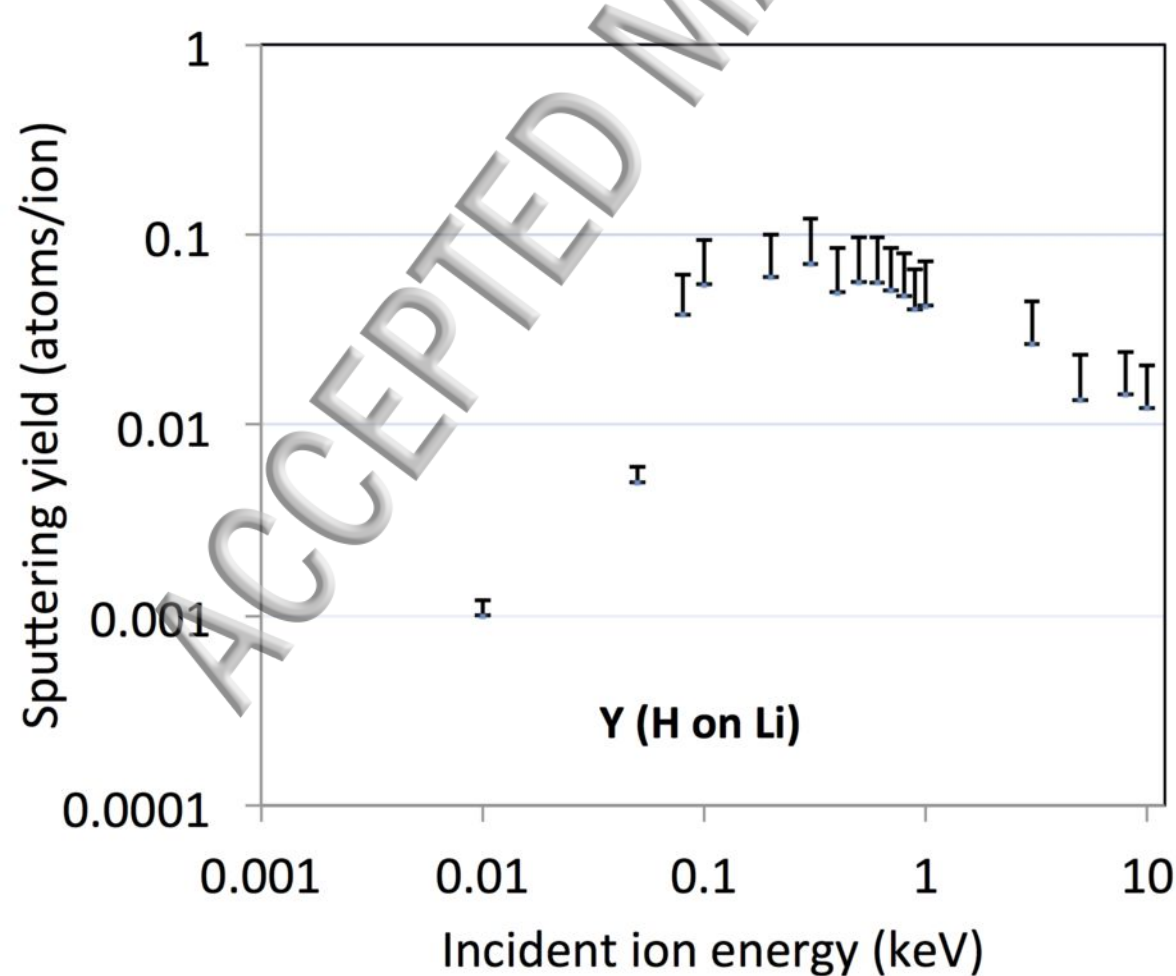


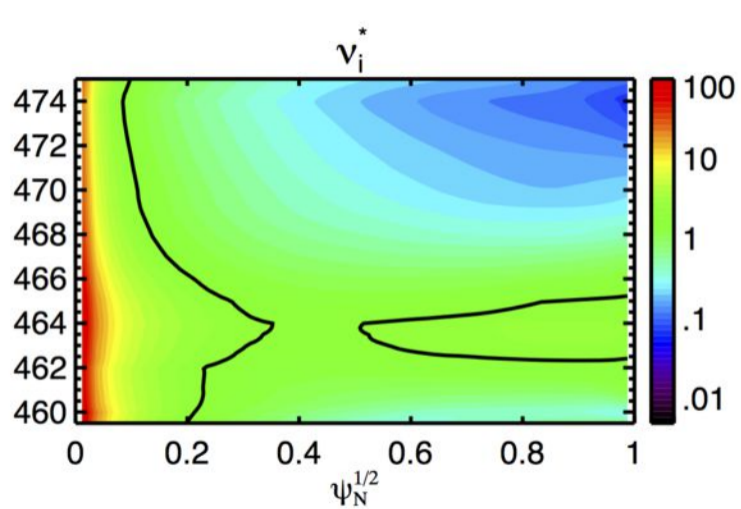
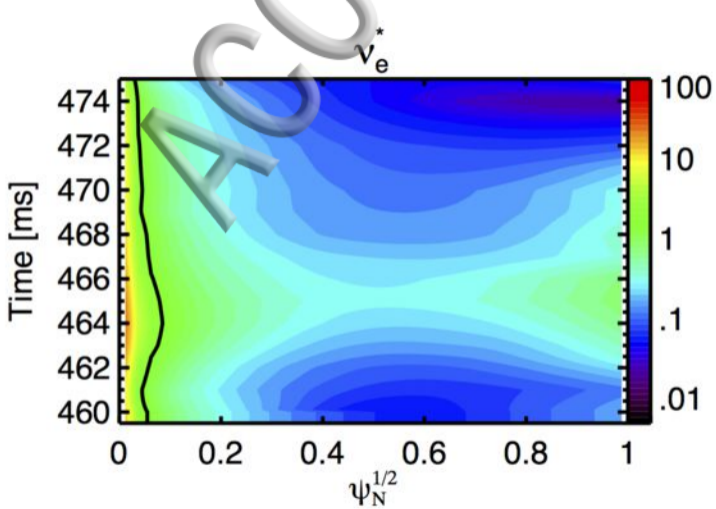


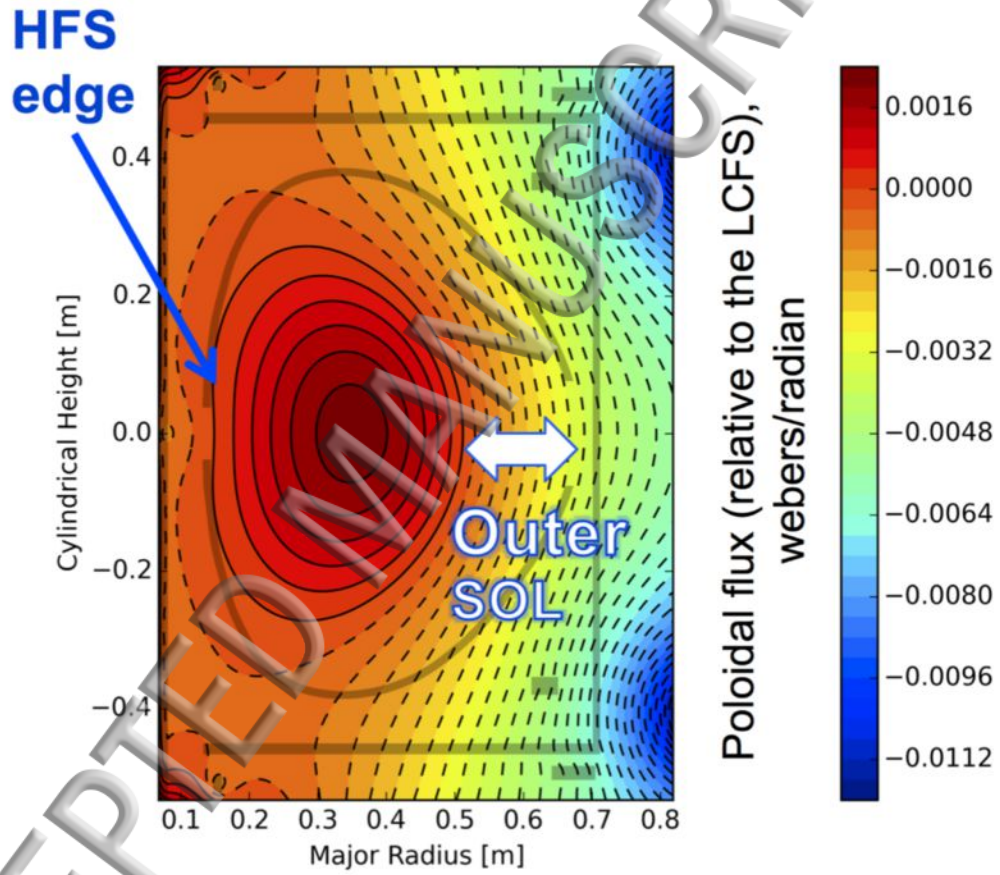














This manuscript was accepted by Phys. Plasmas. Click [here](#) to see the version of record.

